COMMUNICATION

ADVANCED
OPTICAL
MATERIALS

www.advopticalmat.d

Check for updates

Tunable Carbon–CsPbI₃ Quantum Dots for White LEDs

Rafat Rafiei Rad, Andrés. F. Gualdrón-Reyes, Sofia Masi, Bahram Azizollah Ganji, Nima Taghavinia, Santi Gené-Marimon, Emilio Palomares,* and Iván Mora-Seró*

In this work, a simple method to prepare white light emissive diodes based on quantum dot (QD) colloidal solutions using mixed carbon QDs (CQDs) and CsPbI₃ perovskite (PQDs) is reported. The right combination generates emission across the entire visible spectrum upon ultraviolet excitation. The white light emission of the final films provides high and stable color rendering index of 92%, tuning the chromaticity coordinates of the emission through the applied voltage. By varying the CsPbI₃ QD concentration, a mixture is obtained that emits the "warm", "neutral", and "cold" white light sought for many indoor lighting applications, or to approximate the visible region of the solar spectrum, respectively. Remarkably, the material syntheses are low cost and truly scalable. In addition, colloidal mixtures of CQDs and CsPbI₃ PQDs show a facile deposition for light-emitting diode (LED) application, showing white electroluminescence, indicating that both kinds of QDs are stable during LED operation. Last but not least, the photoluminescence quantum yield of the colloidal mixtures is higher (up to 75%) than single white emitters, showing itself as a promising system for white emission with tunable properties.

R. R. Rad, Dr. A. F. Gualdrón-Reyes, Dr. S. Masi, Prof. I. Mora-Seró
Institute of Advanced Materials (INAM)
Universitat Jaume I (UJI)
Avenida de Vicent Sos Baynat, s/n, Castelló de la Plana, Castellón 12071, Spain
E-mail: sero@uji.es
R. R. Rad, Dr. B. A. Ganji
Department of Electrical and Computer Engineering
Babol Noshirvani University of Technology
Babol 484, Iran
Prof. N. Taghavinia
Department of Physics
Sharif University of Technology
Tehran 11155-9161, Iran
Prof. N. Taghavinia
Institute for Nanoscience and Nanotechnology
Sharif University of Technology
Tehran 14588-89694, Iran
S. Gené-Marimon, Prof. E. Palomares
The Institute of Chemical Research of Catalonia – The Barcelona Institute of Science and Technology (ICIQ-BIST)
Tarragona 43007, Spain
E-mail: epalomares@iciq.es
Prof. E. Palomares
ICREA
Passeig Lluís Companys, 23, Barcelona E-08010, Spain

The ORCID identification number(s) for the author(s) of this article can be found under https://doi.org/10.1002/adom.202001508.

White light-emitting diodes (WLEDs) are currently dominating the illumination market and have become a strong contender into the future promising lighting sources for the next generation backlighting components in the display technology.[1,2] The actual strategies for the fabrication of WLEDs consist in the combination of commercial InGaN blue-emitting chips such as back illumination, and yellow converters based on inorganic phosphors doped with lanthanide/rare earths ions such as $YAG:Ce^{3+}$, $Ba_3SiO_5:Eu^{2+}$;[3,4] or of ultraviolet LED coated with red, green and blue phosphors.[5,6] Halide perovskites quantum dots (PQDs) owing to their high photoluminescence quantum yield (PLQY),[7] and tunable bandgap covering the entire visible spectral range and color purity, have reached considerable attention on the development of LEDs.[8–10] However the drawback of the stability remains, as the mixture of halide perovskite produces halide exchange reactions and color instability,[3,11,12] in contrast with chalcogenide QDs.[13] In this context, although PQDs offer a PLQY up to 100% and the color rendering index (CRI) of the PQD mixtures to produce white color can be >80%, the PLQY of the mixture is still far from unity (<70%).[4,14] Clearly, this is an indication that there is a lot of room to improve the white emission. Thus, it is essential to find suitable materials that can provide efficient red, blue, and green (RGB) emission in order to obtain a broadband emission for producing a stable white light. Some alternatives have been adopted to avoid the anion exchange such as the covering of PQDs with SiO_2 composites though sol-gel method, using as $PbSO_4$ coating,[15,16] perhydropolysilazane silica precursor,[11] also poly(methylme thacrylate),[17] polystyrene among others.[18,19] Unfortunately, the PLQY of the PQDs decreases after the covering process in some cases. Additionally, some previous reports have addressed the vulnerability of red-emitting iodide PQDs to the air environment, which causes their fast degradation.[20]

To solve this inconvenient, diverse combination between nanostructured systems such as $CsPbBr_3$ nanoplatelets/$CsPbBr_3$ PQDs/Mn-doped PEA_2PbBr_4 nanosheets[3] and Mn-doped $CsPbCl_3$/Bi-doped Cs_2SnCl_6 PQDs[9] have been employed to fabricate efficient and stable WLEDs. However, by varying the applied voltage in the devices using these systems as active layers, an increase of the corrected color temperatures (CCT) is achieved, but the CRI is simultaneously declined. This fact shows the difficulty of establish a stable high color quality in the wide range of the white color tonalities (from warm to cool), which demands urgently highly stable systems. With

ADVANCED
SCIENCE NEWS
www.advancedsciencenews.com

ADVANCED
OPTICAL
MATERIALS
www.advopticalmat.de

the purpose to ensure the stability of iodide perovskites, as the case of CsPbI$_3$ PQDs, some approaches such as ligand engineering,[21,22] metal doping,[23–25] post-synthetic treatments of PQDs solutions have been performed.[26,27] Recently, we have reported the synthesis of CsPbI$_3$ PQDs with high PLQY > 90%, narrow PL full width at half maximum (FWHM) and long-term stability of 15 months, by varying the conventional hot-injection synthetic protocol.[28] It has been reported that one of the main reason of the high chemical stability of iodide PQDs is attributed to the nanoconfinement provided by their small particle size. In this context, a compressive strain is induced in the perovskite lattice, avoiding the octahedral tilting in the material surface and increasing the surface energy.[29,30] Therefore, the black α-phase of iodide perovskites is thermodynamically preferred over nonphotoactive yellow δ-phase at room temperature, increasing the energy barrier to induce phase transformation.[29,30] Accordingly, the potentiality of CsPbI$_3$ QDs with enhanced photophysical properties can support the development of WLEDs with high and stable CRI.

Moreover, inorganic and less toxic carbon quantum dots (CQDs) have emerged as attractive broad blue light emitters for LEDs fabrication,[31,32] taking advantage of their simple preparation,[33] tunable PL,[34] (similar to PQDs), narrow FWHM and good chemical stability,[31,35] avoiding the photobleaching effect.[36,37] One interesting characteristic of CQDs that has not been widely exploited resides on their ability to generate also a broad PL, reaching the partial coverage of the green region depending on the organic functional groups (chromophores) located on their surface.[38] Although it has been reported that these groups generate carrier energy traps (structural defects) into the CQDs decreasing their PLQY,[31] it is also clear that this broadening of the emission feature can be useful to generate blue-green light switchable by varying the excitation light and

the applied voltage during LED characterization.[32,38] In this context, we have combined blue-green light emitting CQDs with efficient red-emitting and stable PQDs in order to improve the color properties of white emission. Note that the oxygen and ammonium groups (mainly hexylammonium cations in our case) from the CQDs surface generate the PL broadening, covering a portion of the blue and green emissions.[38] In this work, we propose a facile route to produce white-light emitting colloidal solutions by mixing GB-light converter CQDs (10 mg mL^{-1}, PLQY = 21%, see Figure S1, Supporting Information) with different concentrations of R-converter CsPbI$_3$ PQDs (PLQY = 94%), and demonstrate the application in WLED fabrication with tunable warm-cold emission.

Figure S2a,b (Supporting Information) shows the typical TEM images of the CQDs and CsPbI$_3$ PQDs both obtained by hot-injection method (see experimental section in the Supporting Information for more details). CQDs exhibit a spherical morphology, while a nanocube shape is observed for the PQDs. By estimating the corresponding size distribution for each material (Figure S2a',b', Supporting Information), CQDs present an average particle size around 3.6 ± 0.8 nm, while PQDs shows an average particle size around 12.4 ± 1.5 nm.

After mixing the CQDs and different amounts of CsPbI$_3$ PQDs, under UV light ($\lambda = 365$ nm) illumination, the photoluminescence (PL) of the prepared solutions present a broad range of white tonalities, from "cold" to "warm," moving to a predominant red emission when high amount of PQDs are introduced, see **Figure 1**a. All solutions have been prepared with 10 mg mL^{-1} of CQDs and a variable concentration of PQDs, denoted as X-PQDs where X is the concentration in mg mL^{-1}. Samples are denoted based on the concentration of initial solution of QDs used for their preparation as 10-CQDs, 3-PQDs, and X-PQDs, corresponding respectively to only CQDs, only
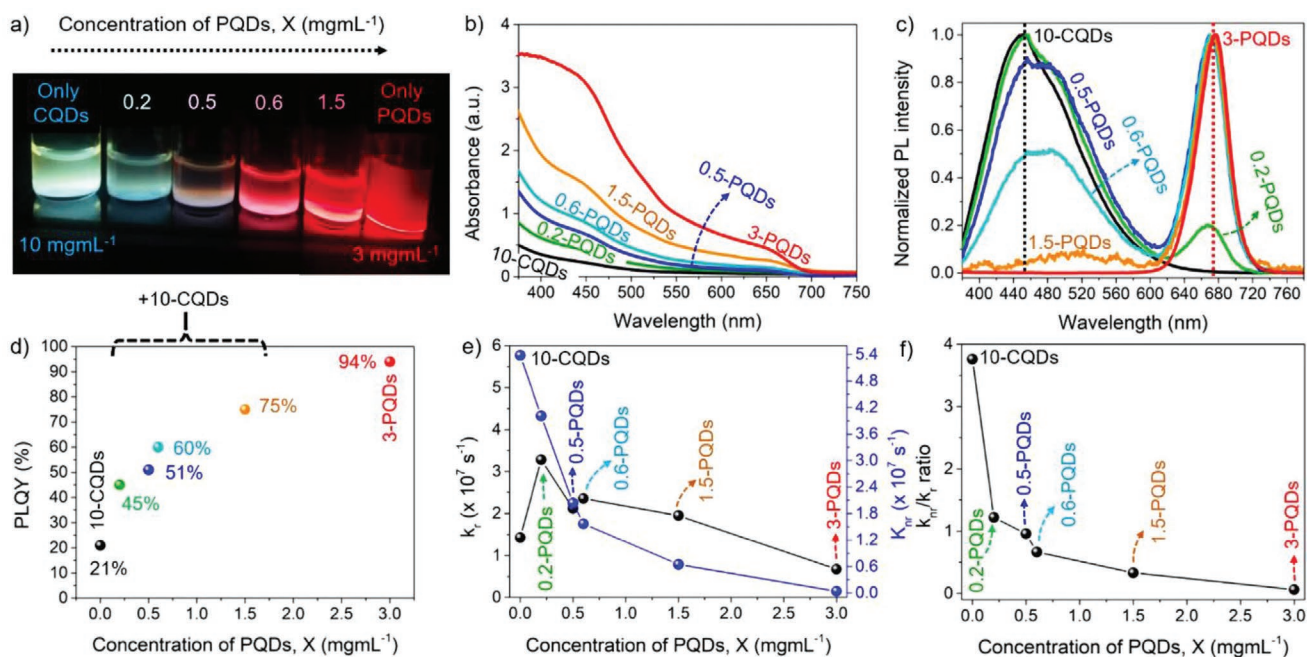

Figure 1. Optical characterization of different solutions with CQDs, PQDs, and mixing both with different ratios by varying the concentration of CsPbI$_3$ PQDs. a) Picture under UV irradiation ($\lambda = 365$ nm), b) UV–vis absorption, c) PL spectra, d) PLQY, e) radiative (k_r) and nonradiative recombination (k_{nr}) decay rate constants, and f) their corresponding k_{nr}/k_r ratio.

PQDs and mixture of 10 mg mL^{-1} CQDs and X mg mL^{-1} PQDs. Figure 1b shows the absorption spectra of the samples containing different rations of CQDs and PQDs, observing the typical absorption edges of CQDs and PQDs around 440 and 650 nm, respectively. The co-existence of these signals probes the absence of secondary reactions between CQDs and PQDs to hamper the degradation of the materials and facilitate the generation of the white emission.

The normalized PL spectra of the different samples are shown in Figure 1c. A broad PL signal with FWHM ≈ 115 nm in the wavelength range between 450 and 530 nm, with a maximum PL peak at 450 nm were obtained for CQDs, while a narrow PL signal with FWHM ≈ 42 nm was achieved for CsPbI$_3$ PQDs. By increasing the amount of PQDs, we evidenced a slight red-shift in the emission peak position from the perovskite, while a substantial decrease and redshift in the PL feature for the CQDs was reached. We attributed the lowering in the PL signal of CQDs to the absorption of PQDs.[39] Since the concentration of CQDs is kept constant, the addition of a higher content of CsPbI$_3$ PQDs ensures a stronger photon absorption by the perovskite and thereby a marked emission in the red region. Therefore, the white color was progressively tuned to a more reddish tonality, see Figure 1a. Another process such as charge carrier transfer between the QDs is also considered to modulate the white-light emission from the colloidal samples (discussed below).

The PLQY of the different solutions are depicted in Figure 1d. A progressive increase of the PLQY is observed as the amount of PQDs increases, as it can be expected from the difference in the PLQY of CQD and PQDs, 21% and 94% respectively, reaching a maximum value of 75% for the 10-CQDs 1.5-PQDs mix solution. Time-resolved PL measurements, see Figure S3a (Supporting Information), have allowed the study of the recombination kinetics of the colloidal mixtures, by calculating their corresponding electron lifetimes, τ_{avg}, see Figure S3b (Supporting Information). The higher the concentration of CsPbI$_3$ PQDs, the higher the τ_{avg}, deducing that the presence of the perovskite defines the carrier recombination process when the presence of CsPbI$_3$ PQDs is important as expected from a low interaction of CQDs and PQDs. Considering the PLQY and τ_{avg} values, radiative and nonradiative recombination decay rate constants, k_r and k_{nr} respectively, are calculated, see Table S1 (Supporting Information). With the lowest PQDs content, 0.2 mg mL^{-1}, k_r was raised up respect pure CQD solution, as consequence of the higher PLQY of PQDs. However, a progressive increase of perovskite concentration produced a slight decrease of k_r, see Figure 1e, due to the increase the reabsorption process as the amount of PQDs is augmented. Interestingly, k_{nr} and consequently k_{nr}/k_r ratio, see Figure 1f, exhibit a continuous reduction as the amount of PQDs is increased in the solutions. This fact is the consequence of the lower nonradiative recombination in CsPbI$_3$ PQDs as them become predominant in the solution.[21,26,28] All these results point to a low interaction between CQDs and PQDs beyond the light reabsorption process. Therefore, we conclude that by tuning the PQDs concentration in mixture with CQDs, the properties of the obtained white color can be tuned by the control of the ratio between both QDs.

On the other hand, time-dependent PL measurements (Figure S4, Supporting Information) were conducted for 24 h

in order to study the stability of the white-emitting 10-CQDs–X-PQDs samples (X = 0.2, 0.5, 1.5); more specifically, the stability of CsPbI$_3$ PQDs in the colloidal mixtures. At the beginning, the intensity of PL peak for PQDs is lower than the PL contribution for CQDs. Nevertheless, after some hours (Figure S4, Supporting Information), the PL signals from both QDs are simultaneously increased when X is 0.5 or 1.5. By considering that there are not reports that explain the above PL trend, we suggest that PQDs improve the radiative recombination of CQDs and mediate the stabilization of white color tonality (cold, neutral or warm) without losing their intrinsic properties. Clearly, although future works can be conducted to elucidate the mechanism to depict the stabilization of CQDs–PQDs, we experimentally observed that CsPbI$_3$ PQDs are stable in the QDs mixtures for a long time, which provides to the colloidal samples a long operational use in optoelectronic applications.

Beyond the photoluminescent behavior of the CQD–PQD mixtures, their potentiality for the preparation of WLEDs with tunable properties was investigated. CQD–PQD mixtures were used as active layers for the WLED fabrication, following the architecture ITO/PEDOT:PSS/poly-TPD/10-CQDs–X-PQDs/TPBi/LiF/Al (X = 0.2, 0.5, 1.5) (see Figure S5a, Supporting Information). As seen in **Figure 2**a–c, we obtained the corresponding electroluminescence (EL) spectra for each WLED device, observing the coverage of all the entire visible region with the combination of the component of Green-Blue emission from CQDs and Red emission from CsPbI$_3$ PQDs. Figure 2d–f shows the LED emitted color, represented in the Commission Internationale de l'Eclairage (CIE) color space, obtained with the different mixtures as function of the applied bias. The central part of the CIE color space, around the center (x = 0.30, y = 0.30), correspond to the white color. The obtained EL was dependent of the PQDs concentration and applied voltage, see Figure 2. Clearly, the CIE, see Figure 2d–f, were shifted to the warm white region after adding more red emitting PQDs.

Note that with the increase of the applied voltage the EL moves from red-warm white to cold white region, as the lower bandgap of PQDs respect CQDs also reduce the threshold potential. Consequently, at low applied voltages the emission mostly arises from PQDs, as it requires lower energy to promote the carrier injection due to their narrow bandgap. This fact can be observed in the band structure of the WLED device (Figure S5b, Supporting Information),[28,40] where the relative conduction and valence bands positions of PQDs show a lower energy separation than those of CQDs. Hence, the radiative recombination can be more easily induced into the perovskite. Then, as applied voltages increase, the emission from CQDs is more clearly manifested. We propose that the low bandgap PQDs are first saturated by carrier injection, and then the carrier injection is favored into the wide bandgap CQDs.

The band structure shown in Figure S5b (Supporting Information) is also useful to gain information about the energy alignment between CQDs–PQDs, showing a type-I structure.[4] The eventual quenching of PL peak of CQDs by adding increasing amount of PQDs (Figure 1c) points to an electron and hole transfer from wide bandgap CQDs to lower bandgap PQDs, modulating and stabilizing the white-light emission from colloidal mixtures. On the other hand, comparing the emission at 6 and 9 V of the different samples in the CIE space
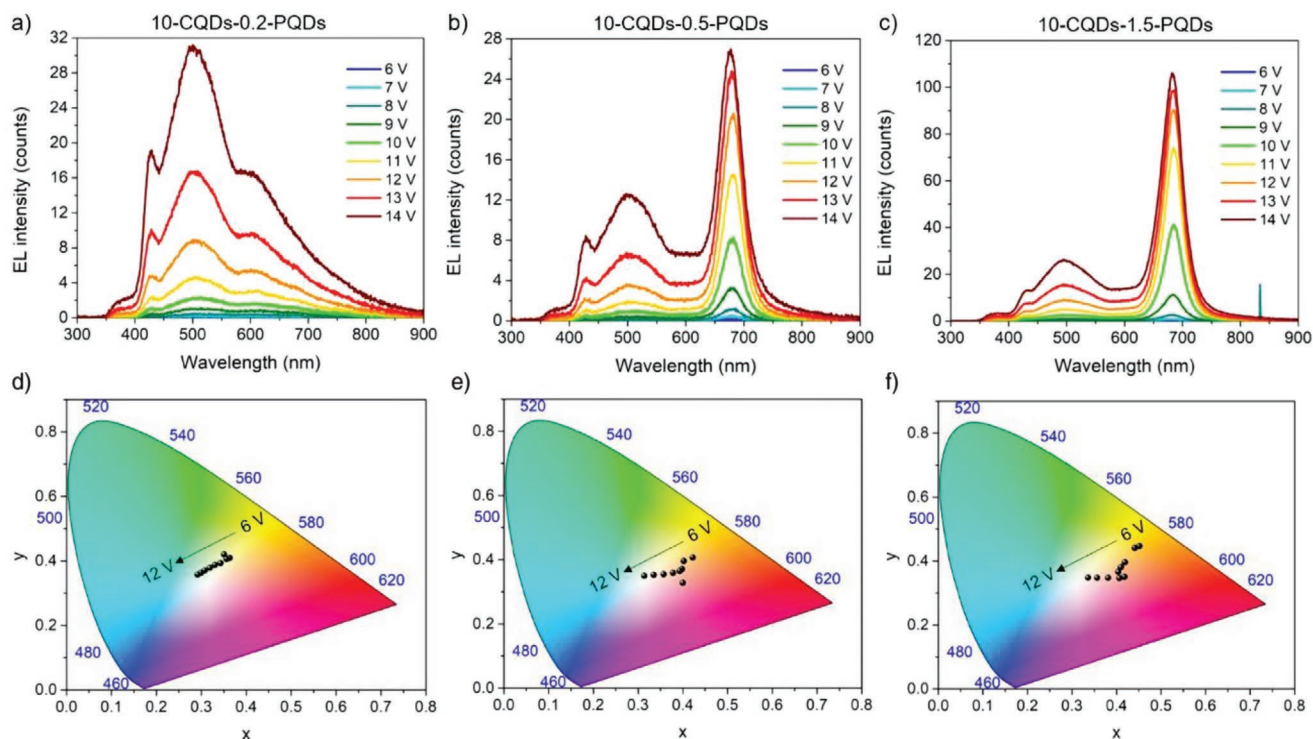
ADVANCED
SCIENCE NEWS
www.advancedsciencenews.com

ADVANCED
OPTICAL
MATERIALS
www.advopticalmat.de

Figure 2. Electroluminescence spectra and their corresponding chromaticity diagram generated by the WLEDs based on 10-CQDs–X-PQDs colloidal solutions, X = 0.2 (a,d), 0.5 (b,e), and 1.5 (c,f) at different operation voltages.

color, the 10-CQDs–0.2-PQDs emission shifts from (0.41,0.44) to (0.29,0.36), see Figure 2d, corresponding to cool white, see Video S1 (Supporting Information). The 10-CQDs–0.5-PQDs emission shifts from (0.33,0.65) to (0.31,0.35), see Figure 2e, corresponding to neutral white, see Video S2 (Supporting Information). The 10-CQDs–1.5-PQDs emission shifts from (0.44,0.44) to (0.34,0.35), see Figure 2f, corresponding to warm white, see Video S3 (Supporting Information). Despite no optimization of the LED at each condition has been performed, a maximum of current density around 1000 mA cm^{-2} was achieved (Figure S5c, Supporting Information), and luminance of 170, 60, 140 Cd m^{-2} have been reported for warm, neutral and cold white emission, see Figure S5d (Supporting Information). However, this demonstration present low external quantum efficiency (EQE), see Figure S5e (Supporting Information), with a wide room for optimization beyond this urgent communication. Some possible reasons to explain the current low performance in the WLEDs come from the degradation of the PQDs/hole transporting layer or PQDs/electron transporting layer as consequence of the presence of the insulating organic capping ligands for both the QDs, high voltages during device operation, environment conditions of heating process during WLED characterization. We also considered the likelihood of an unbalanced carrier transport in the CQD–PQD interface. These issues can hinder the carrier injection at a given potential, decreasing finally the current density and EQE.[13] However, after this proof-of-concept demonstration higher performance can be expected after a systematic optimization process.

In order to highlight the potentiality of this system is worth to present the evolution of CCT and CRI of the WLEDs under operation at different voltages depicted in **Figure 3**a,b,

respectively. For the device using 10-CQDs–0.2-PQDs active layer, the CCT was varied from 3900 to 7300 K, simulating a daylight tonality near to 5183 K. At this point, the CRI was around 92%, indicating the high quality of the white color developed by the CQD–PQD WLED. Additionally, the CRI was maintained ≥88%, deducing that a low concentration of PQDs into the colloidal mixture is enough to provide artificial white light tonalities that can reproduce a wide color gamut compared, for instance, with sunlight. Conversely, the use of 10-CQDs–0.5-PQDs and 10-CQDs–1.5-PQDs displaces the CCT to lower values, inducing the generation of the warm white color with a low CRI. Since CRI of white light is dictated by the combination of RGB-emitters,[42] the excess amount of red emitter reduces the CRI of these samples specially at intermediate applied voltages, see Figure 3b. Interestingly, the sample with the lower amount of CsPbI$_3$ PQDs (x = 0.2) allows a broad range of variation of the CCT with a constant CRI of 90%.[19]

In summary, different solutions have been prepared by mixing in different amounts CQDs and PQDs, observing a low reactivity between both materials in contrast with the anion migration observed when PQD with different composition are mixed. As a consequence, solutions with stable white emission (warm, neutral, cold) have been obtained. The white color emission of the different QD solutions show a combination of the PL range between 420–530 nm with an emission peak at 450 nm from CQDs, and the characteristic PL feature of CsPbI$_3$ PQDs at 675 nm, with a maximum of PLQY ≈ 75% for the 10-CQDs–1.5-PQDs colloidal mixture. We demonstrated the fabrication of WLEDs combining CQDs and PQDs. By modifying the amount of PQDs into 10-CQDs–X-PQDs deposited as an active layer during the fabrication of WLEDs with tuned properties.
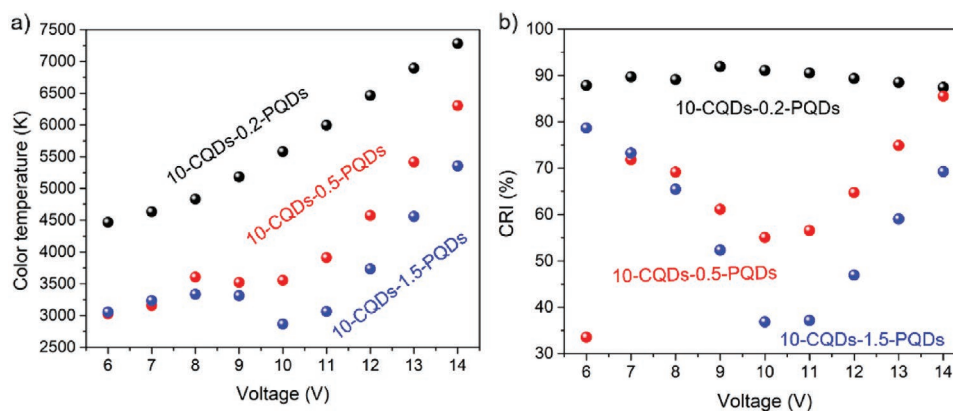
Figure 3. Variation of the a) color temperature and b) color rendering indexes obtained from the WLEDs based on 10-CQDs–X-PQDs colloidal solutions, X = 0.2, 0.5, and 1.5 at different operation voltages.

We obtained a wide CCT range between 3000 and 7500 K (from warm to cold white) depending on the applied bias, with a stable CRI of ~90% for 10-CQDs–0.2-PQDs sample, with a maximum value of 92%, mimicking the daylight. A minimum amount of PQDs is enough to improve the color properties of CQDs WLEDs. These findings offer a new alternative to process in a facile way potential RGB-light emitting QDs solution with suitable photophysical properties that can satisfy the high-quality of white color standards and to be applicable in LED technologies. These results will have important implications in the future development of WLEDs, taking benefit of the enormous potential of both CQDs and PQDs.

Supporting Information

Supporting Information is available from the Wiley Online Library or from the author.

Acknowledgements

Conflict of Interest

The authors declare no conflict of interest.

Author Contribution

R.R.R. and A.F.G.-R. contributed equally to this work. E.P. and I.M.-S. conceived the project. S.G.-M. and A.F.G.-R. synthesized the CQDs and CsPbI$_3$ PQDs, respectively, and performed the corresponding optical properties. R.R.R. and S.M. fabricated the WLEDs devices. B.A.G. and N.T. assisted to the work analysis. E.P. coordinated the CQD synthesis and characterization. I.M.-S. coordinated the solution and WLED preparation, fabrication, and characterization. R.R.R., A.F.G.-R., S.M. and I.M.-S. wrote the manuscript. All the authors contributed to the discussions.

Keywords

[1] X. Dai, Y. Deng, X. Peng, Y. Jin, *Adv. Mater.* **2017**, *29*, 1607022.
[2] Q. Zhou, Z. Bai, W.-g. Lu, Y. Wang, B. Zou, H. Zhong, *Adv. Mater.* **2016**, *28*, 9163.
[3] Z. Gao, X. Wang, Y. Bai, C. Sun, H. Liu, L. Wang, S. Su, K. Tian, Z.-H. Zhang, W. Bi, *Appl. Phys. Lett.* **2019**, *115*, 153103.
[4] Z. Gao, C. Sun, H. Liu, S. Shi, C. Geng, L. Wang, S. Su, K. Tian, Z.-h. Zhang, W. Bi, *Nanotechnology* **2019**, *30*, 245201.
[5] Z. Hao, J. Zhang, X. Zhang, X. Sun, Y. Luo, S. Lu, X.-j. Wang, *Appl. Phys. Lett.* **2007**, *90*, 261113.
[6] J. S. Kim, P. E. Jeon, Y. H. Park, J. C. Choi, H. L. Park, G. C. Kim, T. W. Kim, *Appl. Phys. Lett.* **2004**, *85*, 3696.
[7] M. I. Bodnarchuk, S. C. Boehme, S. ten Brinck, C. Bernasconi, Y. Shynkarenko, F. Krieg, R. Widmer, B. Aeschlimann, D. Günther, M. V. Kovalenko, I. Infante, *ACS Energy Lett.* **2018**, *4*, 63.
[8] C. Y. Kang, C. H. Lin, C. H. Lin, T. Y. Li, S. W. Huang Chen, C. L. Tsai, C. W. Sher, T. Z. Wu, P. T. Lee, X. Xu, M. Zhang, C. H. Ho, J. H. He, H. C. Kuo, *Adv. Sci.* **2019**, *6*, 1902230.
[9] H. Liu, C. Sun, Z. Gao, C. Geng, S. Shi, L. Wang, S. Su, W. Bi, *Nanoscale Res. Lett.* **2019**, *14*, 14.
[10] H. C. Yoon, J. H. Oh, S. Lee, J. B. Park, Y. R. Do, *Sci. Rep.* **2017**, *7*, 7.
[11] D. H. Park, J. S. Han, W. Kim, H. S. Jang, *Dyes Pigm.* **2018**, *149*, 246.
[12] Y. Su, Q. Jing, Y. Xu, X. Xing, Z. Lu, *ACS Omega* **2019**, *4*, 22209.
[13] B. C. Hames, I. Mora-Seró, R. S. Sánchez, *Nano Res.* **2018**, *11*, 1575.
[14] Y. Zheng, X. Yuan, J. Yang, Q. Li, X. Yang, Y. Fan, H. Li, H. Liu, J. Zhao, *J. Lumin.* **2020**, *227*, 117586.
[15] V. K. Ravi, R. A. Scheidt, J. DuBose, P. V. Kamat, *J. Am. Chem. Soc.* **2018**, *140*, 8887.
[16] V. K. Ravi, R. A. Scheidt, A. Nag, M. Kuno, P. V. Kamat, *ACS Energy Lett.* **2018**, *3*, 1049.

ADVANCED
SCIENCE NEWS

www.advancedsciencenews.com

ADVANCED
OPTICAL
MATERIALS

www.advopticalmat.de

[17] C. Sun, X. Shen, Y. Zhang, Y. Wang, X. Chen, C. Ji, H. Shen, H. Shi, Y. Wang, W. W. Yu, *Nanotechnology* **2017**, *28*, 365601.

[18] H. Zhang, X. Wang, Q. Liao, Z. Xu, H. Li, L. Zheng, H. Fu, *Adv. Funct. Mater.* **2017**, *27*, 1604382.

[19] M. Bidikoudi, E. Fresta, R. D. Costa, *Chem. Commun.* **2018**, *54*, 8150.

[20] X. Shen, C. Sun, X. Bai, X. Zhang, Y. Wang, Y. Wang, H. Song, W. W. Yu, *ACS Appl. Mater. Interfaces* **2018**, *10*, 16768.

[21] F. Liu, Y. Zhang, C. Ding, S. Kobayashi, T. Izuishi, N. Nakazawa, T. Toyoda, T. Ohta, S. Hayase, T. Minemoto, K. Yoshino, S. Dai, Q. Shen, *ACS Nano* **2017**, *11*, 10373.

[22] J. Pan, Y. Shang, J. Yin, M. De Bastiani, W. Peng, I. Dursun, L. Sinatra, A. M. El-Zohry, M. N. Hedhili, A.-H. Emwas, O. F. Mohammed, Z. Ning, O. M. Bakr, *J. Am. Chem. Soc.* **2017**, *140*, 562.

[23] X. Shen, Y. Zhang, S. V. Kershaw, T. Li, C. Wang, X. Zhang, W. Wang, D. Li, Y. Wang, M. Lu, L. Zhang, C. Sun, D. Zhao, G. Qin, X. Bai, W. W. Yu, A. L. Rogach, *Nano Lett.* **2019**, *19*, 1552.

[24] F. Liu, C. Ding, Y. Zhang, T. S. Ripolles, T. Kamisaka, T. Toyoda, S. Hayase, T. Minemoto, K. Yoshino, S. Dai, M. Yanagida, H. Noguchi, Q. Shen, *J. Am. Chem. Soc.* **2017**, *139*, 16708.

[25] J.-S. Yao, J. Ge, K.-H. Wang, G. Zhang, B.-S. Zhu, C. Chen, Q. Zhang, Y. Luo, S.-H. Yu, H.-B. Yao, *J. Am. Chem. Soc.* **2019**, *141*, 2069.

[26] F. Li, Y. Liu, H. Wang, Q. Zhan, Q. Liu, Z. Xia, *Chem. Mater.* **2018**, *30*, 8546.

[27] Y. Liu, F. Li, Q. Liu, Z. Xia, *Chem. Mater.* **2018**, *30*, 6922.

[28] E. Hassanabadi, M. Latifi, A. F. Gualdrón-Reyes, S. Masi, S. Y. joon, M. Poyatos, B. Julián-López, I. Mora Seró, *Nanoscale* **2020**, *12*, 14194.

[29] Y. Zhou, Y. Zhao, *Energy Environ. Sci.* **2019**, *12*, 1495.

[30] S. Masi, A. F. Gualdrón-Reyes, I. Mora-Seró, *ACS Energy Lett.* **2020**, *5*, 1974.

[31] F. Yuan, Y.-K. Wang, G. Sharma, Y. Dong, X. Zheng, P. Li, A. Johnston, G. Bappi, J. Z. Fan, H. Kung, B. Chen, M. I. Saidaminov, K. Singh, O. Voznyy, O. M. Bakr, Z.-H. Lu, E. H. Sargent, *Nat. Photonics* **2019**, *14*, 171.

[32] S. Paulo-Mirasol, E. Martínez-Ferrero, E. Palomares, *Nanoscale* **2019**, *11*, 11315.

[33] Y. Ding, F. Zhang, J. Xu, Y. Miao, Y. Yang, X. Liu, B. Xu, *RSC Adv.* **2017**, *7*, 28754.

[34] B. Yuan, S. Guan, X. Sun, X. Li, H. Zeng, Z. Xie, P. Chen, S. Zhou, *ACS Appl. Mater. Interfaces* **2018**, *10*, 16005.

[35] W. Wang, Y. Li, L. Cheng, Z. Cao, W. Liu, *J. Mater. Chem. B* **2014**, *2*, 46.

[36] D. V. Talapin, J. Steckel, *MRS Bull.* **2013**, *38*, 685.

[37] B. Cui, X.-t. Feng, F. Zhang, Y.-l. Wang, X.-g. Liu, Y.-z. Yang, H.-s. Jia, *New Carbon Mater.* **2017**, *32*, 385.

[38] X. Zhang, Y. Zhang, Y. Wang, S. Kalytchuk, S. V. Kershaw, Y. Wang, P. Wang, T. Zhang, Y. Zhao, H. Zhang, T. Cui, Y. Wang, J. Zhao, W. W. Yu, A. L. Rogach, *ACS Nano* **2013**, *7*, 11234.

[39] W. Zhang, D. Dai, X. Chen, X. Guo, J. Fan, *Appl. Phys. Lett.* **2014**, *104*, 091902.

[40] S. Paulo-Mirasol, S. Gené-Marimon, E. Martínez-Ferrero, E. Palomares, *ACS Appl. Electron. Mater.* **2020**, *2*, 1388.

[41] D. Cardenas-Morcoso, A. F. Gualdrón-Reyes, A. B. Ferreira Vitoreti, M. García-Tecedor, S. J. Yoon, M. Solis de la Fuente, I. Mora-Seró, S. Gimenez, *J. Phys. Chem. Lett.* **2019**, *10*, 630.

[42] P. Zhu, H. Zhu, G. C. Adhikari, S. Thapa, *OSA Continuum* **2019**, *2*, 1880.